Disruption of dNTPs Homeostasis by Ribonucleotide Reductase Hyperactivation Overcomes AML Differentiation Blockade

Hanying Wang, Xin He, Lei Zhang, Haojie Dong, Feiteng Huang, Jie Xian, Min Li, Wei Chen, Xiyuan Lu, Khyatiben V. Pathak, Wenfeng Huang, Zheng Li, Lianjun Zhang, Le Xuan Truong Nguyen, Lu Yang, Lifeng Feng, David Gordon, Jing Zhang, Patrick Pirrotte, Chun-Wei Chen, Amandeep Salhotra, Ya-Huei Kuo, David Horne, Guido Marcucci, David Sykes, Stefano Tiziani, Hongchuan Jin, Xian Wang, Ling Li

Supplemental Methods

Cell culture

293T cells were cultured in DMEM medium with 10% FBS and 1% penicillin/streptomycin (Gibco). The human AML cell lines U937, KG1A, MOLM13, NB4 and THP1 (ATCC) were cultured in RPMI 1640 medium with 10% FBS and 1% penicillin/streptomycin. TF-1_IDH2^{R140Q} cells were generated by infecting TF-1 with MSCV-based retrovirus containing full-length IDH2^{R140Q} and maintained in RPMI 1640 medium with 10% FBS and 1% penicillin/streptomycin. Human normal CD34^{+} and primary AML cells were maintained in StemSpan Serum-Free Expansion Media (SFEM, StemCell Technologies) supplemented with 50 ng/mL of recombinant human stem cell factor (hSCF), 100 ng/mL of Fms-like tyrosine kinase 3 ligand (hFlt3L), 100 ng/mL of thrombopoietin (hTPO), 25 ng/mL of interleukin-3 (hIL-3), and 10 ng/mL of interleukin-6 (hIL-6) (Peprotech Inc.). Murine MA9-transformed cells or MA9/Kras^{G12D} cells were cultured in SFEM supplemented with murine growth factors (mIL-3, 10 ng/mL; mIL-6, 10 ng/mL; mSCF, 30 ng/mL). Lys-GFP-ER-HoxA9 (ER-HoxA9) cells were maintained as described previously [1]. Briefly, this murine GMP-like line was cultured in RPMI 1640 supplemented with 10% FBS, 1% penicillin/streptomycin, and mSCF (100 ng/mL). β-estradiol (Sigma) was added to a final concentration of 0.5 μM from a 10 mM stock dissolved in 100% ethanol. Cells were grown at 37°C in a humidified atmosphere containing 5% CO_2.

Flow-cytometry based differentiation screen

In brief, ER-HoxA9 cells (5,000 cells) were seeded in a volume of 200 μl in each well of a tissue-culture-treated 96-well plate. Compounds were added to the well to a final concentration of 5 μg/mL. Following a 4-day incubation, cells were analyzed by using a BD LSRII flow cytometer. Live cells were discriminated from dead cells based on DAPI staining. Differentiation was assayed by measuring GFP^{+} percentages.

In vitro differentiation

Human AML lines or primary AML cells were seeded in 24-well plates and treated with compounds as indicated. After stained with flow cytometry antibodies (CD11b: APC or PE-Cy7, CD14: PerCP/Cyanine5.5, CD15: FITC or BV421, CD38: FITC or BV510), cells were resuspended in FACS buffer containing 1 μg/mL DAPI and analyzed on LSRII or Fortessa X20 flow cytometer (BD).

Mass cytometry

Primary cells were treated as indicated and processed according to the Fluidigm Maxpar protocol using Maxpar reagents. After viability staining by Cell-ID Cisplatin, cells were incubated with a mixture of customized metal-conjugated surface marker antibodies. After fixation and intercalation, samples were acquired on a Helios mass cytometer (Fluidigm). Mass cytometry data were normalized using EQ Four Element Calibration Beads (Fluidigm). tSNE analyses were performed using Cytobank Premium (Cytobank Inc.).

Real-time quantitative PCR analysis

RNA was isolated using Trizol reagent (Invitrogen) and purified using Direct-zol™ RNA Microprep kits (Zymo Research) according to the manufacturers' protocols. First-strand cDNA was generated using high-capacity cDNA reverse transcription kits (Applied Biosystems). Quantitative real-time PCR was performed using TaqMan® fast advanced master mix (Life Technologies) with Taqman probes, or SYBR Green master mix (Life Technologies) with gene-specific primers. Signals were detected with a QuantStudio 7 Flex Real-Time PCR system (Applied Biosystems). Relative expression levels were determined by normalizing to GAPDH levels. Taqman probes for GAPDH (Hs02786624_g1) and myeloid differentiation transcription factors according to previous reports [2], i.e., CEBPA (Hs00269972_s1), SPI1 (Hs00231368_m1), GFI1 (Hs00382207_m1), EGR1 (Hs00152928_m1) and EGR2 (Hs00166165_m1) were purchased from Thermo Fisher Scientific. Primers for RRM1 (F: GTGTGGGAAATCTCTCAGA, R: CCATGGCTGCTGTGTT), RRM2 (F: AGGGGCTCAGCTTGG, R: GGGGCAGCTGCTTTAG), RRM2B (F: AGAGGCTCGCTGTTTCTATGG, R: GCAAGGCCCAATCTGCTTTTT), DUSP6 (F: GAACTGTGGTGTCTTGGTACATT, R: GTTCATCGACAGATTGAGCTTCT) and GAPDH (F: GTCGGAGTCAACGGATT, R: AAGCTTCCCGTTCTCAG) were synthesized from Integrated DNA Technologies, Inc.

Morphological analysis

For Wright-Giemsa staining, cytospins were prepared by diluting 200,000 cells in 100 µl PBS and spinning onto glass slides using a cytocentrifuge (CytoSpin 4, 900 rpm, 10 min). Cells were fixed in absolute methanol, stained in Wright-Giemsa stain solution (Thermo Fisher Scientific), and rinsed in pH 6.6 phosphate buffer. Images were acquired and analyzed under an INFINITY 2 microscope camera (Lumenera) and imaging software. Morphological signs of differentiation include decreased cytoplasmic basophilia, nuclear lobulation, cytoplasmic granularity and reduced nucleus/ cytoplasm ratio [3]. For monocyte-specific α-naphthyl acetate esterase activity assay, cytospins were prepared as described above, and α-naphthyl acetate esterase activity was evaluated using the LEUCOGNOST® EST kit (Millipore) according to the manufacturer's instructions. Briefly, slides were fixed in LEUCOGNOST® Fixing Mixture prior to incubation in freshly prepared staining solution in the dark. After counterstaining with Mayer's hemalum solution, slides were rinsed and air-dried, and then assessed under microscope. Red-brown granular color in monocytes indicated α-naphthyl acetate esterase activity [4]. For nitroblue tetrazolium (NBT) reduction assay, 200,000 live cells were washed with PBS, centrifuged, and resuspended in 500 µl complete medium containing 1 mg/mL NBT and 500 ng/mL phorbol 12-myristate 13-acetate (PMA) (both from Sigma-Aldrich). After incubation in the dark at 37 °C for 30 min, cells were washed with PBS, spun onto slides, and examined for insoluble blue-black deposits (nitroblue diformazan) under microscope [5].

Western blotting

Cells were lysed in buffer containing 50 mM Tris (pH 7.4), 150 mM NaCl, 1 mM EDTA, 0.5% NP-40, and 0.5% sodium deoxycholate, supplemented with protease and phosphatase inhibitors. Boiled lysates were resolved on sodium dodecyl sulfate-polyacrylamide gel electrophoresis (SDS-PAGE) gels and transferred to nitrocellulose membranes (Bio-Rad). Proteins of interest were sequentially probed with primary and secondary antibodies. Horseradish peroxidase-conjugated secondary antibodies were from Jackson ImmunoResearch Laboratories (Westgrove, PA). Antibody detection was performed with SuperSignal™ West Pico or Femto chemiluminescent substrates (Thermo Fisher Scientific). Results were imaged by G: BOX Chemi XX6 gel doc systems (Syngene) and visualized using GeneSys image acquisition software (Syngene). Protein levels were determined by densitometry with ImageJ software (NIH, Bethesda, MD) if necessary.

Drugs, reagents and DNA constructs

Nelarabine for in vivo administration was purchased from DC Chemical Inc. (Shanghai). Cytarabine was purchased from City of Hope Pharmacy. BCI hydrochloride was purchased from Axon Medchem (Reston). COH29 was synthesized and purified by Dr. David Horne's lab at City of Hope. All the other agents if not specified and for in vitro treatment were purchased from Cayman Chemical (Ann Arbor). All the antibodies were obtained from commercial sources. Phospho-CHK1 (S345), phospho-CHK2 (T68), GAPDH, ERK1/2, phospho-ERK1/2 (T202/T204) antibodies were from Cell Signaling Technology. RRM1, RRM2, E2F1, CCNF antibodies were from Genetex. SAMHD1 antibody was from Proteintech. β-actin, R2/p53R2 antibodies were from Santa Cruz Biotechnology. DUSP6 antibody was from MyBioSource. γH2AX and FLAG antibody were from Millipore Sigma. Mouse monoclonal S9.6 antibody was from Kerafast. Rabbit polyclonal V5 tag antibody was from Abcam. Alexa 488-conjugated mouse anti-ERK1/2 (pT102/pY204) and IgG isotype control were purchased from BD Biosciences. V5-tagged RNASEH1 expression vector (MigRI-NLS-hRNaseH1 WT-V5) was kindly provided by Dr. Donger Zhang [6]. Inducible shRRM2 as well as control shRNA vector were from Transomic Technologies as previously reported [7]. Flag-tagged RRM2-WT, RRM2-T33A, RRM2-Rxl/AxA cDNAs were synthesized and cloned into PCDH-EF1A-IRES-GFP vector (Genscript). Flag-tagged inducible RRM2-Rxl/AxA mutant, as well as MOCK vector was modified from a previous reported inducible RRM2-T33A expression vector from Dr. David Gordon's lab [7]. MISSION shRNA bacterial glycerol stocks were purchased from Millipore Sigma. pLKO-U6-shRNA-PGK-puro vectors were engineered into pLKO-U6-shRNA-SF-DsRed vectors as previously described [8] if necessary. Targeting sequences were as follows: shCCNF-1, TCAGGCCAGGAAGTCATGTTT; shCCNF-2, TCAGGCCAGGAAGTCATGTTT; shE2F1, CGCTATGAGACCTCACTGAAT; shERK2-1, TATTACGACCCGAGTGACGAG; shERK2-2, TGGAATTGGATGACTTGCCTA; and shScramble, GCGCGCTTTGTAGGATTCG. Oligonucleotides encoding for DUSP6 gRNAs were CACCGGACGACTCGTATAGCTCCTG (fwd) and AAACCAGGAGCTATACGAGTCGTCC (rev). Oligonucleotides encoding for non-targeting control gRNAs were CACCGGATTCTAAAACGGATTACCA (fwd) and AAACTGGTAATCCGTTTTAGAATCC (rev).

Lentivirus production and transduction

Replication-incompetent lentiviruses were obtained as described previously [8,9]. Briefly, 293T cells were transiently transfected with pMD2.G envelope plasmids, psPAX2 packaging plasmids as well as specific lentivectors for gene overexpression or knockdown by calcium-phosphate co-

precipitation. Supernatants containing virus particles were harvested, filtered, and concentrated using PEG. In the case of lentiviral vectors expressing indicated shRNAs or indicated cDNAs, cells were exposed to virus-containing supernatants (MOI=1 for cell lines, MOI=20 for primary AML cells) in the presence of 8 μg/mL polybrene via spinoculation, and then sorted by flow cytometry based on RFP/GFP expression or selected by puromycin (2 μg/mL). For primary cell transduction, cells were stimulated in SFEM supplemented with high concentrations of growth factors as described above, followed by two exposures to virus-containing supernatants in the presence of TransDux (System Biosciences) via spinoculation.

Retrovirus production and transduction

The MLL-AF9 retroviral vectors were transfected into 293T cells using TransIT®-LT1 Transfection Reagent (Mirus) together with pCL-ECO packaging plasmids. Lineage negative cells were enriched for splenocytes isolated from $Kras^{LSL\ G12D/+}$/Vav-Cre^{+} mice or Vav-Cre^{+} mice as control and incubated overnight in serum free medium supplemented with mIL-3 (10 ng/mL), mIL-6 (10 ng/mL) and mSCF (100 ng/mL). After incubation, cells were infected with retrovirus in the presence of 8 μg/mL polybrene in retronectin-coated plates via two rounds of spinoculation.

Generation of SAMHD1 KO CRISPR–Cas9 cells

Oligonucleotides encoding for SAMHD1 gRNAs were CACCGCTCGGGCTGTCATCGCAACG (fwd) and AAACCGTTGCGATGACAGCCCGAGC (rev) as described previously [10]. Oligos were annealed and cloned into the ipUSEPR lentiviral sgRNA vector (hU6-driven sgRNA co-expressed with EF-1α-driven RFP and puromycin-resistance gene) using the BsmBI restriction sites [11]. After lentivirus production and titration, Cas9-expressing THP1 cells were transduced at an estimated multiplicity of infection (MOI) of 1 in the presence of 8 μg/mL polybrene via spinoculation. Transduced bulk cells were selected with 2 μg/mL puromycin and subjected to single cell isolation by flow cytometry. Individual single-cell clones with disrupted SAMHD1 expression were identified by western blot. Genomic DNA was prepared using QuickExtract™ DNA Extraction Solution (Lucigen) according to manufacturer's protocol. Clones were then genotyped by sequencing of genomic DNA using the following primers: ACTGCCCTCAGTTCTGCTTC (fwd) and AGATCCCAATCTACGACTG (rev).

Orthotopic AML mouse model

AML cell lines, and T-cell depleted or $CD34^{+}$ AML specimens were transplanted via tail vein injection into sub-lethally irradiated (180 cGy) 6-8-week-old NSGS mice as described previously

[12]. Nelarabine (43.4 mg/mL) was administrated intravenously through tail vein in a volume of 5 µl per gram of body weight, which yielded 217 mg/kg as reported [13]. Cytarabine was administrated intraperitoneally at a dose of 50 mg/kg daily for 14 consecutive days [10]. BCI was administrated intraperitoneally at a dose of 10 mg/kg twice daily for two weeks [14]. For the induction chemotherapy treatment, Ara-C and DNR (daunorubicin) were reconstituted with PBS, filtered, and stored in aliquots at -20 °C. The chemotherapy regimen consists of a daily dose of 50 mg/kg Ara-C (i.p.) for five consecutive days along with a daily dose of 3 mg/kg DNR (i.v.) during the first three days of Ara-C treatment as described previously [15]. Weights were taken daily during treatment and doses were recalculated upon drug administration. For patient derived xenograft (PDX) models treated with nelarabine, mice were euthanized at 12 weeks post transplantation, and bone marrow contents of femurs were assessed for long-term engraftment and in vivo differentiation by labeling with anti-human CD45, CD33, CD34, CD117, CD14, CD64, CD15, CD49d antibodies, followed by flow cytometry analysis.

Limiting dilution assays

For in vitro limiting dilution assays (LDAs), MA9$^+$ primary murine AML cells or primary AML CD34$^+$ cells were cultured in methylcellulose medium with recombinant cytokines containing dG (15 µM) and plated in 48-well plates at a limiting dilution manner. For each dose, 12 wells were included. The number of wells containing spherical colonies was counted after 7 days. For in vivo LDA, engineered MA9$^+$ murine AML cells were injected into sublethally irradiated B6.SJL (CD45.1$^+$) recipient mice via tail vein at a limiting dilution manner. The number of recipient mice developed full-blown leukemia within two months post transplantation was counted from each group. ELDA software [16] was utilized to evaluate the frequency of LSCs.

BM transplant using Samhd1 KO mouse

Genotyping primers and relevant PCR protocols for Samhd1$^{-/-}$ mouse are reported previously [17]. For RRM2 transduction, BM c-Kit$^+$ cells from Mll-AF9/Samhd1$^{-/-}$ mouse were transduced with lentiviral vectors expressing iRxI/AxA construct. After puromycin selection in ColonyGEL methylcellulose medium with murine recombinant cytokines, cells were collected and injected into sublethally irradiated B6.SJL (CD45.1$^+$) recipient mice (200,000 donor cells per recipient) via tail vein. Doxycycline induction (i.g., 10 mg/kg, daily) started 2 weeks after transplantation. CD45.2$^+$ donor cells in BM were detected on Day 30 post doxycycline induction and sorted by flow cytometry for western blot or primer extension assay.

Mitochondrial explorations

Mitochondrial superoxide and membrane potential were detected by using MitoSOX and MitoTracker CMXRos, respectively (Thermo Fisher Scientific; Cat # M36008, Cat # M7512), according to manufacturer's instructions. Quantification of cytosolic and mitochondrial resident mtDNA using DLoop2 primers was performed as previously reported [18]. For transmission electron microscopy (TEM), cells were fixed with 2.5% glutaraldehyde in 0.1 M cacodylate buffer ($Na(CH_3)_2AsO_2 \cdot 3H_2O$), pH 7.2, at 4°C. Cell pellets were secondary fixed with 2% osmium tetroxide, serially dehydrated with ethanol and embedded in Eponate [19]. Ultra-thin sections (70 nm thick) were acquired by ultramicrotomy, post-stained, and examined on an FEI Tecnai 12 transmission electron microscope equipped with a Gatan OneView CMOS camera. TEM images were taken at nominal 11,000× magnification.

In vivo bioluminescence imaging

AML cell line xenograft models of systemic disease were established as described previously [9]. Briefly, U937, THP1 and MOLM13 cells were infected with lentiviral vectors expressing luciferase reporter plus GFP and then sorted based on GFP positivity for intravenous inoculation into NSGS mice. For in vivo bioluminescence imaging, mice were injected intraperitoneally with 150 mg/kg D-luciferin (Goldbio) dissolved in PBS solution, and then anesthetized with isoflurane, followed by imaged with Lago X (Spectral Instruments Imaging). The bioluminescent signals were quantified using Aura imaging software (Spectral Instruments Imaging). Total flux values were determined by drawing regions of interest and are presented as photons/second/cm^2/steradian.

Immunofluorescence assays

Cells were collected, washed in ice-cold PBS and spun onto glass slides using a cytocentrifuge (CytoSpin 4, 900 rpm, 10 min). Cells were fixed with 4% paraformaldehyde, permeabilized with 0.2% Triton X-100, blocked with 3% BSA and incubated with primary rabbit anti-RRM2 antibody or mouse anti-DNA-RNA Hybrid S9.6 antibody. Slides were then incubated with secondary goat anti-rabbit Alexa 488 antibody or goat anti-mouse Alexa 594 antibody (Life technologies). Nuclei were counterstained with ProLong™ Gold Antifade Mountant with DAPI (Thermo Fisher Scientific). Images were acquired using a Zeiss confocal laser-scanning-microscope (Zeiss LSM 880 with Airyscan). ImageJ software was used to integrate the nuclear S9.6 signal for quantitative analysis.

Intracellular staining for phospho-ERK

Phospho-ERK1/2 analysis was performed as reported previously with modifications [20]. Briefly, cells were harvested, fixed in 2% paraformaldehyde, permeabilized in methanol at -20 °C overnight, and further labeled with diluted conjugated antibody and isotype control. Data were acquired on Fortessa X20 or LSRII flow cytometer.

Analysis of viability, apoptosis, cell cycle and colony growth

Cell growth was measured using the Cell Titer-Glo Luminescent Cell Viability Assay Kit (Promega) in accordance with the manufacturer's instructions. Results were expressed as percentages of control from three replicates. Apoptosis was assessed by Annexin V/DAPI staining followed by flow cytometry. Cell cycle was analyzed by Ki-67/DAPI staining based on the manufacturer's protocol (BD Biosciences). Colony formation capacity based on colony forming cell number was determined in methylcellulose progenitor assays as described [12,21]. For serial replating of engineered MA9$^+$ murine AML cells, colony cells were collected and replated every 7 days. Colony formation units were counted and compared for each passage.

Cell synchronization

For synchronization at G_1/S, cells were incubated with 2 μM aphidicolin for 24 hours, washed and incubated in fresh aphidicolin-free medium for 12 hours and then incubated with 2 μM aphidicolin for additional 24 hours, as described previously [22]. This 60-h double-aphidicolin treatment blocked the cells at the G_1/S boundary. For G_2/M phase enrichment, cells were treated with 100 ng/mL nocodazole for 16 hours [23].

Genome-wide CRISPR/Cas9 knockout library screen

Human GeCKO v2 CRISPR knockout pooled library (A and B, Addgene: 1000000048 and 1000000049) was used as described [24,25]. First, we established a stable Cas9-expressing U937/R cell line (U937/R-Cas9) by lentiviral transduction of Cas9 coding sequence (Addgene: 52962) followed by blasticidin selection (10 μg/mL). The optimal function of Cas9$^+$ clone was confirmed by lentiviral transduction of a self-excising tagRFP sgRNA construct (sg_tRFP657_294). Next, we transduced cells with lentivirus carrying pooled guide RNA at a low MOI (~0.2) to ensure effective barcoding of individual cells. 24 hours post transduction, cells were selected with 2 μg/ml puromycin for consecutive 7 days to generate a mutant cell pool, which was then treated with vehicle and NEL (20 μM) for additional 7 days, respectively. Baseline points were harvested 2 days post puromycin selection. After treatment, 3.6×10^7 cells per replicate (2 replicates in total)

were collected for genomic DNA extraction to ensure over 300× coverage of library. The integrated sgRNA sequences were PCR-amplified using DreamTaq HotStart Green 2x Master Mix (primer: Fwd- CTTGTGGAAAGGACGAAACACCG, Rev- GTGGATGAATACTGCCATTTGTCT) and subjected to massive parallel amplicon sequencing carried out by COH core facility. The sgRNA read count and hits calling were analyzed by MAGeCK algorithm [26,27]. The magnitude and significance of gene depletion based on guide RNA drop-out were interpreted as fold change and *P* value, respectively; both of which were taken into accounts for calculation of a negative score.

Correlation analyses of pharmacogenomics screen data

Pearson correlations between basal gene expression and NEL or Ara-C sensitivity for hematopoietic and lymphoid-tissue-derived cell lines were determined using Prism 9 (GraphPad Software). mRNA expression data were obtained from the Cancer Cell Line Encyclopedia (http://www.broadinstitute.org/ccle) [28], and NEL or Ara-C AUC measurements were obtained from the Cancer Therapeutics Response Portal (https://ocg.cancer.gov/programs/ctd2/data-portal) [29,30] or Genomics of Drug Sensitivity in Cancer (https://www.cancerrxgene.org/) [31-33].

Metabolomic analysis

Cells were treated with drugs as indicated for 12 hours. For isotope labeling, cells were cultured in RPMI 1640 medium with 10% dialyzed FBS, 1% streptomycin/penicillin and 11.1 mM $^{13}C_6$ glucose (Cat# CLM-1396-1, Cambridge Isotope Laboratories) or 2 mM $^{15}N_1$ glutamine (Cat# NLM-557-1, Cambridge Isotope Laboratories). Metabolites were extracted with cold 80% methanol followed by centrifugation at 4°C. The supernatant was collected and evaporated to dryness on Vacufuge Plus (Eppendorf) at 30°C. Metabolites were resuspended in 50% acetonitrile (ACN) and subjected to targeted metabolomic analysis on the UltiMate 3000 UPLC chromatography system coupled with a Thermo Scientific Q Exactive mass spectrometer. The chromatographic separation was achieved on a Luna 3u NH2 100A (150× 2.0 mm) column (Phenomenex), and performed on a Vanquish Flex (Thermo Scientific) with 5 mM NH_4AcO (pH 9.9, mobile phase A) and ACN (mobile phase B) at a flow rate of 200 µl/min. The linear gradient from 15% A to 95% A over 18 min was followed by an isocratic step at 95% A for 9 min and re-equilibration. The Q Exactive mass spectrometer was run with polarity switching (+3.5 kV/−3.5 kV) in full scan mode with an m/z range of 70-975 and 70.000 resolution. TraceFinder 4.1 (Thermo Scientific) was used to quantify targeted metabolites by area under the curve (AUC) using accurate mass measurements (±3 ppm) and expected retention times. Data were normalized to the cell number.

Relative amounts of metabolites were calculated by summing up the values for all isotopologues of a given metabolite. To plot the heatmap, the detection levels for all metabolites were further transformed by Z-score normalization.

Measurement of intracellular nucleotides by quantitative LC-MS/MS analysis

Cells were treated as indicated in RPMI 1640 medium with 10% dialyzed FBS. Nucleotides were extracted using 100 µl ice-cold methanol/acetonitrile (50% V/V) containing stable isotopically labelled internal standards followed by three freeze-thaw cycles (freeze 30 seconds in liquid nitrogen, and thaw by sonication at 4°C for 30 min). Proteins were precipitated by centrifugation at 13,000 rpm for 15 min at 4°C; supernatants were then further diluted using 400 µL of water. The clear metabolite extract was immediately used for analysis on a Vanquish UHPLC coupled to a TSQ Altis triple quadrupole mass spectrometer (Thermo Fisher Scientific). The separation was performed using a Hypercarb™ column (100 mm x 2.1 mm, 5 µm) (Thermo Fisher Scientific) with a 12 min gradient as previously descried [34]. The injection volume was 10 µL. Mass spectrometry analysis was performed using multiple reaction monitoring in negative ionization mode, with parameters as follows: spray voltage at 2600, sheath gas at 60, auxiliary gas at 15, sweep cone at 2, ion transfer tube temperature at 380 °C and vaporization temperature at 350 °C. The optimized collision energy and RF lens values for each of analytes are summarized in the table below.

Compound	Precursor (m/z)	Product (m/z)	Collision Energy (V)	RF Lens (V)
UMP	322.9	78.9	32.52	85
UMP	322.9	96.8	21.68	85
UMP	322.9	211.2	16.26	85
S-AMP	462.2	78.9	32.18	128
S-AMP	462.2	97	23.23	128
S-AMP	462.2	134	41.73	128
dCTP	465.95	158.9	25.85	94.31
dCTP	465.95	367.98	20.61	94.31
dCTP	465.95	386	23.5	94.31
dUTP	467	158.9	32.29	106.18
dUTP	467	368.9	19.86	106.18
dUTP	467	387	22.47	106.18

dTTP	481.2	158.9	30.66	105.43
dTTP	481.2	256.95	28.73	105.43
dTTP	481.2	384	20.5	105.43
CTP	482.1	78.9	50	105
CTP	482.1	159	30	105
Ara-CTP	482.2	78.9	50	105
Ara-CTP	482.2	159	30	105
UTP	483	79	30	105
UTP	483	159	30	105
IMP	347	78.8	26.42	103
IMP	347	79	32.75	103
IMP	347	211	15.69	103
GMP	362.1	78.9	30.09	92
GMP	362.1	211.1	18.95	92
ADP	426	79	40	128
ADP	426	134.1	40	128
ADP	426	158.8	28.69	128
dGDP	426.1	79	40	128
GDP	442.1	78.9	37.07	131
GDP	442.1	344.1	16.67	131
dGTP	506	158.9	28.92	98.76
dGTP	506	408	21.07	98.76
dGTP	506	426	23.91	98.76
ATP	506.1	78.9	49.96	89
ATP	506.1	159	29.37	89
ATP	506.1	408	19.4	89
GTP	522	78.9	55	140
GTP	522	150	41.5	140
GTP	522	158.9	37.6	140
Ara-GTP	522.1	78.9	55	105
Ara-GTP	522.1	158.9	31.27	105
Ara-GTP	522.1	176.9	23.12	105
ADO_IS	273	136	17.81	65
AMP	346.1	78.9	24.22	110

dATP	490	158.9	28.39	90.98
dATP	490	392	21.98	90.98
dATP	490	410	24.25	90.98
$^{13}C_{10}$,$^{15}N_5$-ATP	521	78.9	49.96	89
$^{13}C_{10}$,$^{15}N_5$-ATP	521	159	29.37	89
$^{13}C_{10}$,$^{15}N_5$-ATP	521	423	19.4	89

Ara-GTP and Ara-CTP standards were purchased from TriLink Biotechnologies (San Diego, CA). dTTP was purchased from Santa Cruz Biotechnology (Dallas, TX). All the other listed analytes and internal standards (Adenosine-$^{13}C_{10}$,$^{15}N_5$-5′-triphosphate and Adenosine-$^{13}C_5$) were purchased from Sigma-Aldrich (St. Louis, MO). Stock and working solutions were prepared in LC-MS grade water. A ten-point calibration curve and quality controls at low, medium and high concentration were prepared in analyte-free matrix at 0.01 to 12 nmoles/1x10^6 cells. Analyte-free cell matrix was generated using charcoal activation [35]. Calibration curves showed excellent linearity (all correlation coefficient of > 0.99) with accuracy and precision within 15%.

Measurement of dNTP by PCR-based primer extension assay

Following indicated treatments, 5×10^6 cells were harvested and resuspended in ice-cold 60% methanol. Cell pellets were vortexed vigorously, boiled for 3 min and the extracts were centrifuged at 4°C at 16,000 g for 20 min. Supernatants were filtered through pre-equilibrated Amicon Ultra-0.5-ml centrifugal filters (Millipore, MA) at 4°C and dried at 70°C using a vacuum centrifuge. Pellets were resuspended in nuclease-free water and stored at −80°C until use. Reaction mixtures contained primer, probe and template at an equimolar final concentration of 0.4 µmol/L. $MgCl_2$ was included at a final concentration of 2 mmol/L. Non-limiting dNTPs were included in the reaction mix in excess at a final concentration of 100 µmol/L (the dNTP to be assayed was excluded). AmpliTaq Gold DNA polymerase was added at 0.875 U/reaction, 2.5 µl of 10x PCR Buffer II added and nuclease-free ddH_2O added to a final reaction volume of 25 µl. For analysis of cell extracts, the volume of ddH_2O was modified to accommodate the addition of 2.5 µl of cell extract. Thermal profiling and fluorescence detection were performed using the 'isothermal' program on board an Applied Biosystems 7500 Real-Time PCR System. For analysis of dNTPs, the thermal profile consisted of a 10 min 95°C step to 'hot-start' the *Taq* polymerase and a primer extension time of up to 30 min at 60°C. Raw fluorescence spectra for 6-FAM were measured using filter A at specified time intervals (typically every 5 min) to follow assay progression using Sequence Detection Software (SDS Version 1.4, Applied Biosystems) and exported and analyzed

in Microsoft Excel and Prism 9. In all cases, fluorescence values for blank reactions (limiting dNTP omitted) were subtracted to give normalized fluorescence units (NFUs) to account for background probe fluorescence. A detailed protocol has been previously described [36].

RNA-Seq analysis

Total RNA was isolated from cells using Trizol Reagent (Life technologies) following the manufacturer's instructions. RNA sequencing libraries were prepared with Kapa RNA HyperPrep kit (Kapa Biosystems, Cat KR1352) with poly(A)-enriched protocol. Sequencing run was performed in the single read mode using Illumina HiSeq 2500. Sequenced reads were aligned to the human hg38 reference genome with TopHat2 (v 2.0.14). Gene expression levels were quantified using HTSeq (v 0.6.1). The counts data were normalized using the trimmed mean of M values (TMM) method, implemented in the Bioconductor package edgeR (v.3.30.3) to obtain the normalized RPKM (Reads Per Kilobase of transcript, per Million mapped reads) value. The differential expression analysis was also performed using edgeR (v.3.30.3). The enrichment analysis was performed using Gene Set Enrichment Analysis (GSEA, v.4.0.3) and Ingenuity Pathway Analysis (IPA, v.62089861).

Statistical analysis of patient cohorts

In GSE14468 AML cohort of 526 patients, only 262 patients had overall survival data, out of which 246 had NRAS/KRAS gene mutation annotations, including 219 RAS wildtype (NRAS/KRAS double negative) and 27 RAS mutated (either KRAS or NRAS) patients. mRNA expression levels were log2 transformed normalized intensity for Affymetrix U133 plus 2.0 array downloaded from GEO database. In TCGA AML cohorts of 200 patients, only 163 patients treated with cytarabine were analyzed, out of which 147 had mRNA sequencing data. The gene expression levels were log2 transformed RPKM. Kaplan-Meier curves were used for survival analysis and log-rank test was used to test the difference between groups. To assess the risk associated with the mRNA levels of RRM2, Cox proportional hazard model was used, with *P* values for hazard ratios calculated by the Wald test. Both univariate and multivariate analyses were run with or without adjustment for age and gender.

Statistical methods

The variability of CD11b expression or cell viability affected by two factors, e.g., RRM2 KD/OE and drug treatment, or CCNF KD and RRM2 KD was analyzed with two-way ANOVA with multiple comparisons. The cell growth after CCNF KD, RRM2 OE or drug treatment across four days, was

analyzed with two-way ANOVA with repeated measures. The IC_{50} values between shCtrl and shCCNF were analyzed by means of Extra-sum-of-squares F test. Gene expression levels and drug AUC were analyzed with Pearson correlation test. Kaplan-Meier survival for animal studies were analyzed with Mantel-Cox log-rank test. All the statistical analyses were performed using Prism 9 (GraphPad).

References

1. Sykes DB, Kfoury YS, Mercier FE, et al. Inhibition of Dihydroorotate Dehydrogenase Overcomes Differentiation Blockade in Acute Myeloid Leukemia. *Cell*. 2016;167(1):171-186.e115.
2. Tenen DG, Hromas R, Licht JD, Zhang D-E. Transcription Factors, Normal Myeloid Development, and Leukemia. *Blood*. 1997;90(2):489-519.
3. Lainey E, Wolfromm A, Sukkurwala AQ, et al. EGFR inhibitors exacerbate differentiation and cell cycle arrest induced by retinoic acid and vitamin D3 in acute myeloid leukemia cells. *Cell Cycle*. 2013;12(18):2978-2991.
4. Sokol RJ, Hudson G, Wales JM, Goldstein DJ, James NT. Quantitative enzyme cytochemistry during human macrophage development. *J Anat*. 1993;183 (Pt 1):97-101.
5. Collins SJ, Ruscetti FW, Gallagher RE, Gallo RC. Normal functional characteristics of cultured human promyelocytic leukemia cells (HL-60) after induction of differentiation by dimethylsulfoxide. *J Exp Med*. 1979;149(4):969-974.
6. Chen L, Chen JY, Huang YJ, et al. The Augmented R-Loop Is a Unifying Mechanism for Myelodysplastic Syndromes Induced by High-Risk Splicing Factor Mutations. *Mol Cell*. 2018;69(3):412-425.e416.
7. Koppenhafer SL, Goss KL, Terry WW, Gordon DJ. Inhibition of the ATR–CHK1 Pathway in Ewing Sarcoma Cells Causes DNA Damage and Apoptosis via the CDK2-Mediated Degradation of RRM2. *Molecular Cancer Research*. 2020;18(1):91.
8. Li L, Wang L, Li L, et al. Activation of p53 by SIRT1 inhibition enhances elimination of CML leukemia stem cells in combination with imatinib. *Cancer Cell*. 2012;21(2):266-281.
9. Li L, Osdal T, Ho Y, et al. SIRT1 activation by a c-MYC oncogenic network promotes the maintenance and drug resistance of human FLT3-ITD acute myeloid leukemia stem cells. *Cell Stem Cell*. 2014;15(4):431-446.
10. Herold N, Rudd SG, Ljungblad L, et al. Targeting SAMHD1 with the Vpx protein to improve cytarabine therapy for hematological malignancies. *Nature Medicine*. 2017;23(2):256-263.
11. Liu Q, Chan AKN, Chang WH, et al. 3-Ketodihydrosphingosine reductase maintains ER homeostasis and unfolded protein response in leukemia. *Leukemia*. 2022;36(1):100-110.
12. Sun J, He X, Zhu Y, et al. SIRT1 Activation Disrupts Maintenance of Myelodysplastic Syndrome Stem and Progenitor Cells by Restoring TET2 Function. *Cell Stem Cell*. 2018;23(3):355-369.e359.
13. Perry JM, Tao F, Roy A, et al. Overcoming Wnt-β-catenin dependent anticancer therapy resistance in leukaemia stem cells. *Nat Cell Biol*. 2020;22(6):689-700.

14. Kesarwani M, Kincaid Z, Gomaa A, et al. Targeting c-FOS and DUSP1 abrogates intrinsic resistance to tyrosine-kinase inhibitor therapy in BCR-ABL-induced leukemia. *Nature Medicine*. 2017;23(4):472-482.

15. Jiang X, Hu C, Ferchen K, et al. Targeted inhibition of STAT/TET1 axis as a therapeutic strategy for acute myeloid leukemia. *Nat Commun*. 2017;8(1):2099.

16. Hu Y, Smyth GK. ELDA: extreme limiting dilution analysis for comparing depleted and enriched populations in stem cell and other assays. *J Immunol Methods*. 2009;347(1-2):70-78.

17. Rehwinkel J, Maelfait J, Bridgeman A, et al. SAMHD1-dependent retroviral control and escape in mice. *Embo j*. 2013;32(18):2454-2462.

18. Wu HC, Rerolle D, Berthier C, et al. Actinomycin D targets NPM1c-primed mitochondria to restore PML-driven senescence in AML therapy. *Cancer Discov*. 2021.

19. Mascorro JA, Bozzola JJ. Processing biological tissues for ultrastructural study. *Methods Mol Biol*. 2007;369:19-34.

20. Kong G, You X, Wen Z, et al. Downregulating Notch counteracts KrasG12D-induced ERK activation and oxidative phosphorylation in myeloproliferative neoplasm. *Leukemia*. 2019;33(3):671-685.

21. He X, Zhu Y, Lin YC, et al. PRMT1-mediated FLT3 arginine methylation promotes maintenance of FLT3-ITD(+) acute myeloid leukemia. *Blood*. 2019;134(6):548-560.

22. Rodriguez CO, Gandhi V. Arabinosylguanine-induced Apoptosis of T-Lymphoblastic Cells. *Cancer Research*. 1999;59(19):4937.

23. D'Angiolella V, Donato V, Forrester FM, et al. Cyclin F-mediated degradation of ribonucleotide reductase M2 controls genome integrity and DNA repair. *Cell*. 2012;149(5):1023-1034.

24. Sanjana NE, Shalem O, Zhang F. Improved vectors and genome-wide libraries for CRISPR screening. *Nature Methods*. 2014;11(8):783-784.

25. Shalem O, Sanjana NE, Hartenian E, et al. Genome-scale CRISPR-Cas9 knockout screening in human cells. *Science*. 2014;343(6166):84-87.

26. Li W, Köster J, Xu H, et al. Quality control, modeling, and visualization of CRISPR screens with MAGeCK-VISPR. *Genome Biology*. 2015;16(1):281.

27. Li W, Xu H, Xiao T, et al. MAGeCK enables robust identification of essential genes from genome-scale CRISPR/Cas9 knockout screens. *Genome Biology*. 2014;15(12):554.

28. Barretina J, Caponigro G, Stransky N, et al. The Cancer Cell Line Encyclopedia enables predictive modelling of anticancer drug sensitivity. *Nature*. 2012;483(7391):603-607.

29. Rees MG, Seashore-Ludlow B, Cheah JH, et al. Correlating chemical sensitivity and basal gene expression reveals mechanism of action. *Nat Chem Biol*. 2016;12(2):109-116.
30. Seashore-Ludlow B, Rees MG, Cheah JH, et al. Harnessing Connectivity in a Large-Scale Small-Molecule Sensitivity Dataset. *Cancer Discov*. 2015;5(11):1210-1223.
31. Yang W, Soares J, Greninger P, et al. Genomics of Drug Sensitivity in Cancer (GDSC): a resource for therapeutic biomarker discovery in cancer cells. *Nucleic Acids Research*. 2012;41(D1):D955-D961.
32. Iorio F, Knijnenburg TA, Vis DJ, et al. A Landscape of Pharmacogenomic Interactions in Cancer. *Cell*. 2016;166(3):740-754.
33. Garnett MJ, Edelman EJ, Heidorn SJ, et al. Systematic identification of genomic markers of drug sensitivity in cancer cells. *Nature*. 2012;483(7391):570-575.
34. Zhu B, Wei H, Wang Q, et al. A simultaneously quantitative method to profiling twenty endogenous nucleosides and nucleotides in cancer cells using UHPLC-MS/MS. *Talanta*. 2018;179:615-623.
35. Thakare R, Chhonker YS, Gautam N, Alamoudi JA, Alnouti Y. Quantitative analysis of endogenous compounds. *J Pharm Biomed Anal*. 2016;128:426-437.
36. Wilson PM, Labonte MJ, Russell J, Louie S, Ghobrial AA, Ladner RD. A novel fluorescence-based assay for the rapid detection and quantification of cellular deoxyribonucleoside triphosphates. *Nucleic Acids Res*. 2011;39(17):e112.

Supplemental Tables

Supplemental Table S1. The common genes upregulated by ATRA in HL60, Kasumi1, MOLM13 and MV4-11. (Related to Figure 1)

See attached Excel Table S1 (Supplementary spreadsheet)

Supplemental Table S2. The common up-regulated genes shared by signatures of 3 differentiation-induction compounds. (Related to Figure 1)

See attached Excel Table S2 (Supplementary spreadsheet)

Supplemental Table S3. Top 79 candidate chemicals showing significant positive correlations with CD38 level in the NCI-60 collection. (Related to Figure 1)

See attached Excel Table S3 (Supplementary spreadsheet)

Supplemental Table S4. Clinical information relevant to primary AML samples. (Related to Figure 1)

ID	Type	Risk	Status	Gene mutation	Cyto.	WBC (k)	% Blast (PB, BM)	Used in Figure
1	PB	P	R	ITD, NPM1	ND	62.3	88, ND	1E, 1F, 1H, 1I, 1J, 1K, S1F, S1I, S1J, S1K, S1M, 2O, 2P, 2Q, 2R, S2L, S2Z, 3A, 3B, S3N, 4J, 4K, S5M, S5N
2	PB	B	U	ASXL1, RUNX1	NK	NA	48, 84	S1E, S1I, S1J, 2F, 3I, S3I, 4J, 4K, S5A, 6J, S6H
3	PB	I	U	FLT3, IDH1, NPM1, SRSF2	NK	NA	87, 95	S1E, S1I, S1J, 2F, 3I, 4J, 4K, S4J, S4K, S5A, S5B, 6J, S6H
4	PB	B	U	CEBPA, KMT2C, SUZ12	NK	NA	80, 60	S1E, S1I, S1J, 2F, 3I, 4J, 4K, S4J, S4K, 5F, 5G, 5M, S5E, S5F, S5G, 6J, 6K, S6H
5	PB	I	U	NRAS	inv (3)	NA	24, 30	S1E, S1I, S1J, 2F, S2U, S2V, 3I, 4J, 4K, S5A
6	PB	P	R	CEBPA, KIT, TET2, WT1	CK	NA	50, 32	1H, S1E, S1I, S1J, 2F, 2L, S2V, 3I, 4J, 4K,

								S4J, S4K, S5A, S5B
7	PB	P	U	No	del (5)	41.4	60, 90	1H, S1E, S1I, S1J, S1K, S2L
8	BM	P	R	KRAS, NRAS, U2AF1, ITD	NK	73.5	ND, 39	1F, 1H, 1J, 1K, S1E, S1I, S1J, S1K, S1M, S2L
9	BM	I	U	PTPN11, NRAS, NPM1	NK	23.7	ND, 58	S1I
10	BM	B	U	BCOR, RUNX1, WT1, KRAS, NRAS	NK	4	ND, 58	S1I
11	PB	P	U	No	CK	22.3	71, 86	S1I
12	PB	P	R	ITD, TKD	Trisomy 8	32.7	40, 65	S1I, S2U, S2V
13	BM	I	U	NRAS	del (5)	6.1	ND, 90	S1I
14	BM	P	R	TET2, KRAS, DNMT3A	CK	105	34, ND	S1I, S2U, S2V
15	BM	P	R	NRAS, KMT2D	CK	6.5	ND, 80	S1I
16	BM	P	U	ITD	NK	86.3	90, 90	S1I
17	PB	P	U	ITD	Trisomy 8	263.5	90, 90	S1I
18	PB	P	R	CBFB, TP53	CK	184.9	90, 80	S1I

Abbreviations: Cyto., cytogenetics; BM, bone marrow; PB, peripheral blood; B, better-risk; I, intermediate-risk; P, poor-risk; U, untreated; R, relapsed; ITD, FLT3-ITD; TKD, FLT3-TKD; ND, not determined; NK, normal karyotype; CK, complex karyotype; NA, not available.

Supplemental Table S5. Metabolite intensities in U937, KG1A cells treated with NEL or vehicle control. (Related to Figure 2)

See attached Excel Table S5 (Supplementary spreadsheet)

Supplemental Table S6. The AUC intensity values of each metabolite isotopologue from ^{13}C-glucose tracing experiment in U937 cells treated with NEL or vehicle control. (Related to Figure 2)

See attached Excel Table S6 (Supplementary spreadsheet)

Supplemental Table S7. The AUC intensity values of each metabolite isotopologue from amide-^{15}N-glutamine tracing experiment in U937 cells treated with NEL or vehicle control. (Related to Figure 2)
See attached Excel Table S7 (Supplementary spreadsheet)

Supplemental Table S8. RPKM values and differential gene expression analyses result of NEL-treated U937 cells versus vehicle control from 4 replicates. (Related to Figure 5)
See attached Excel Table S8 (Supplementary spreadsheet)

Supplemental Table S9. RPKM values and differential gene expression analyses result of NEL-treated KG1A cells versus vehicle control from 4 replicates. (Related to Figure 5)
See attached Excel Table S9 (Supplementary spreadsheet)

Supplemental Table S10. RPKM values and differential gene expression analyses result of dG-treated U937 cells versus vehicle control from duplicates. (Related to Figure 5)
See attached Excel Table S10 (Supplementary spreadsheet)

Supplemental Table S11. RPKM values and differential gene expression analyses result of dG-treated KG1A cells versus vehicle control from duplicates. (Related to Figure 5)
See attached Excel Table S11 (Supplementary spreadsheet)

Supplemental Table S12. RPKM values and differential gene expression analyses result of engineered iRxl/AxA THP1 cells versus MOCK control following DOX treatment from 4 replicates. (Related to Figure 5)
See attached Excel Table S12 (Supplementary spreadsheet)

Supplemental Table S13. Hazard rates for mRNA levels of RRM2 in GSE14468 cohort of patients with RAS mutant or RAS wildtype AML. (Related to Figure 5)

mRNA	RAS WT patients		RAS mutant patients	
	OS[a]	OS[b]	OS[a]	OS[b]
RRM2	0.79	0.83	**0.28**	**0.26**
	(0.55-1.13; 0.20)	(0.58-1.18; 0.30)	**(0.10-0.83; 0.02)**	**(0.09-0.76; 0.01)**

Abbreviations: OS, overall survival.

Superscript a [(a)] indicates data from univariate analysis; superscript b [(b)] indicates data adjusted for age and gender. Shown are hazard rates, 95% confidence intervals and *P* values calculated with Wald test. Bold text indicates *P* values <0.05.

Supplemental Table S14. Normalized gene-level CRISPR negative scores of NEL-treated cells versus vehicle control from duplicates, respectively. (Related to Figure 6)

See attached Excel Table S14 (Supplementary spreadsheet)

Supplemental Figures

Supplemental Figure 1

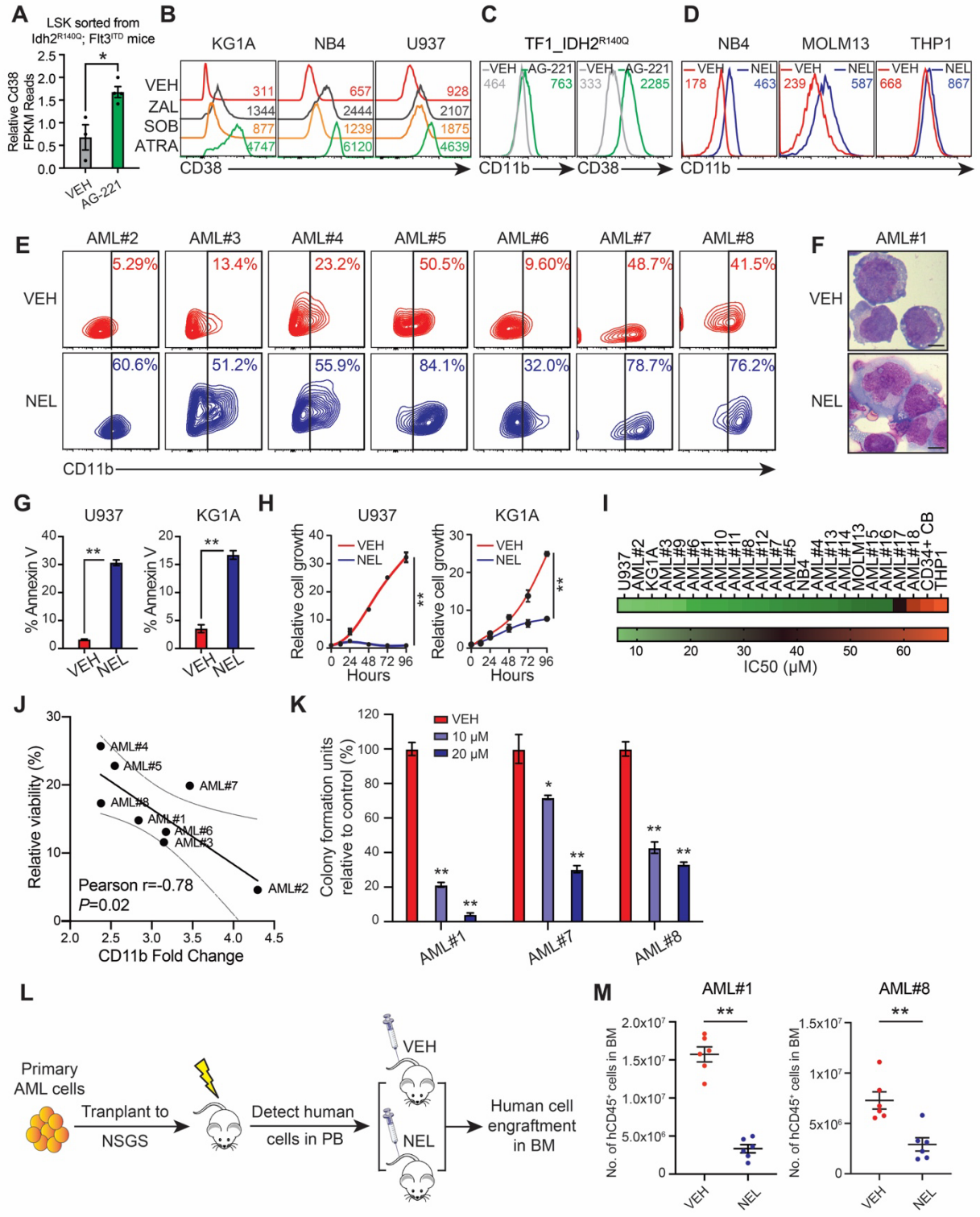

Figure S1. A functional screen reveals a differentiation-induction activity of nelarabine (Related to Figure 1)

(A) FKPM reads of Cd38 expression in LSK subset sorted from $Idh2^{R140Q}$; $Flt3^{ITD}$ mice treated with either vehicle or AG-221 (GSE78691). Results represent the mean ± SEM, and * P<0.05.

(B) CD38 expression levels in indicated AML cell lines following treatment with vehicle, zalcitabine (ZAL, 2 μM), sodium butyrate (SOB, 1 mM) and ATRA (1 μM) for 96 hours.

(C) CD38 and CD11b expression levels in TF1_$IDH2^{R140Q}$ cells treated with vehicle or AG-221 (1 μM, 96 hours).

(D-E) CD11b expression levels in indicated AML lines (D) or primary AML cells (E) after NEL treatment (20 μM, 96 hours).

(F) Representative morphological changes in primary AML $CD34^+$ cells from specimen AML#1 after NEL treatment (20 μM, 96 hours) by Wright-Giemsa staining. Scale bar, 5 μm.

(G-H) Apoptosis (G) and relative cell growth (H) of U937 or KG1A cells treated with NEL (10 μM, 96 hours) based on Annexin V/DAPI labeling or CellTiter Glo assay, respectively. Results represent the mean ± SEM, and ** P<0.01.

(I) IC_{50} of AML cell lines and primary AML cells following NEL treatment based on CellTiter Glo assay.

(J) Pearson correlation analysis between CD11b expression fold changes and relative viability in a panel of primary AML cells after NEL treatment (20 μM, 96 hours).

(K) CFC assay of primary AML cells (n=3) treated with vehicle or NEL (20 μM, 7 days). Results represent the mean ± SEM. * P<0.05, and ** P<0.01.

(L) Schematic illustration of leukemic PDX model transplanted with $CD34^+$ or T-cell depleted AML cells from primary specimens administrated with NEL (217 mg/kg, i.v., daily) or vehicle (PBS). Mice were sacrificed 12 weeks post-BMT for analyses of human cell engraftment and in vivo differentiation.

(M) Number of human $CD45^+$ cells in BM of NSGS mice xenografted with AML specimens (#1 or #8) and treated as indicated. Results represent the mean ± SEM, and ** P<0.01.

Supplemental Figure 2

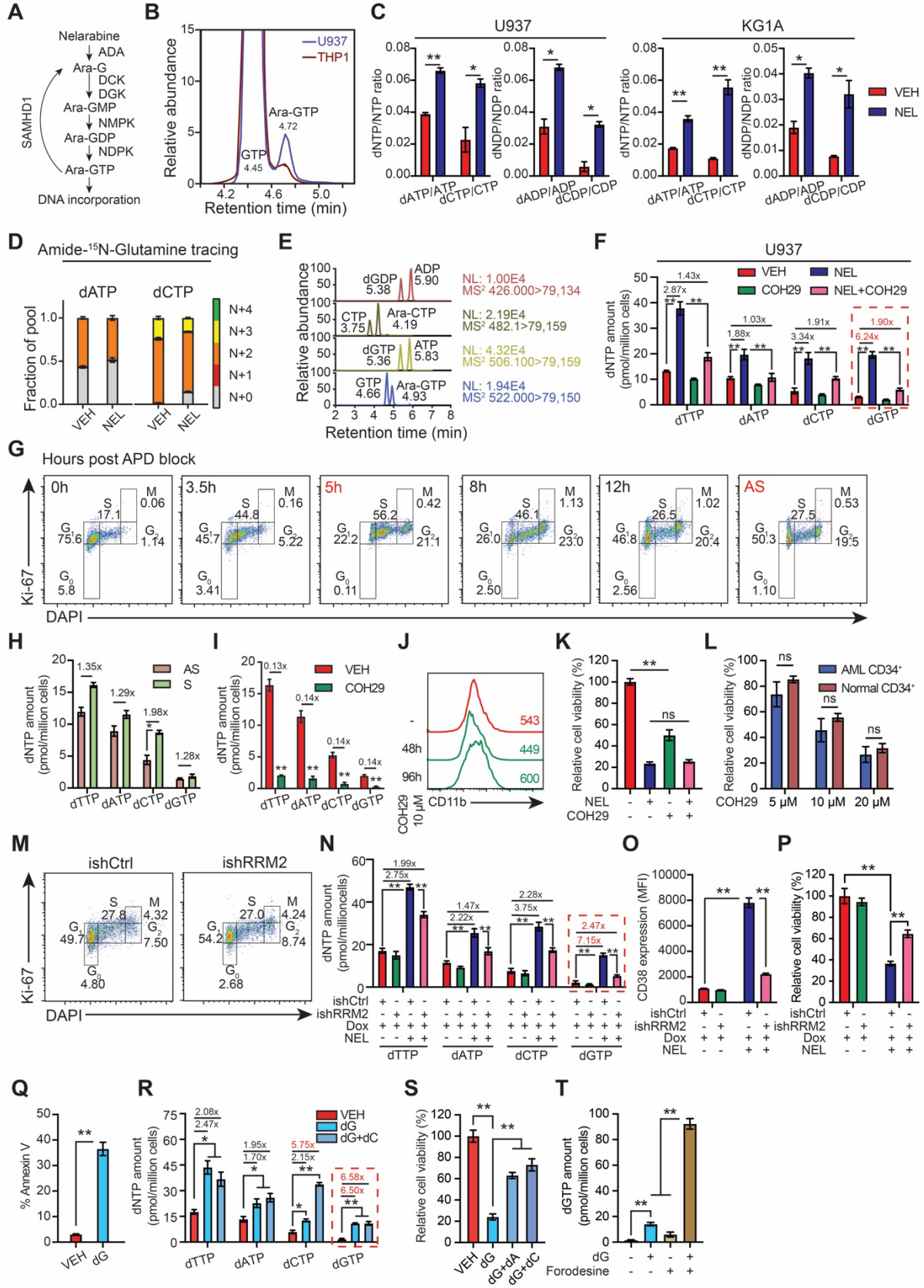

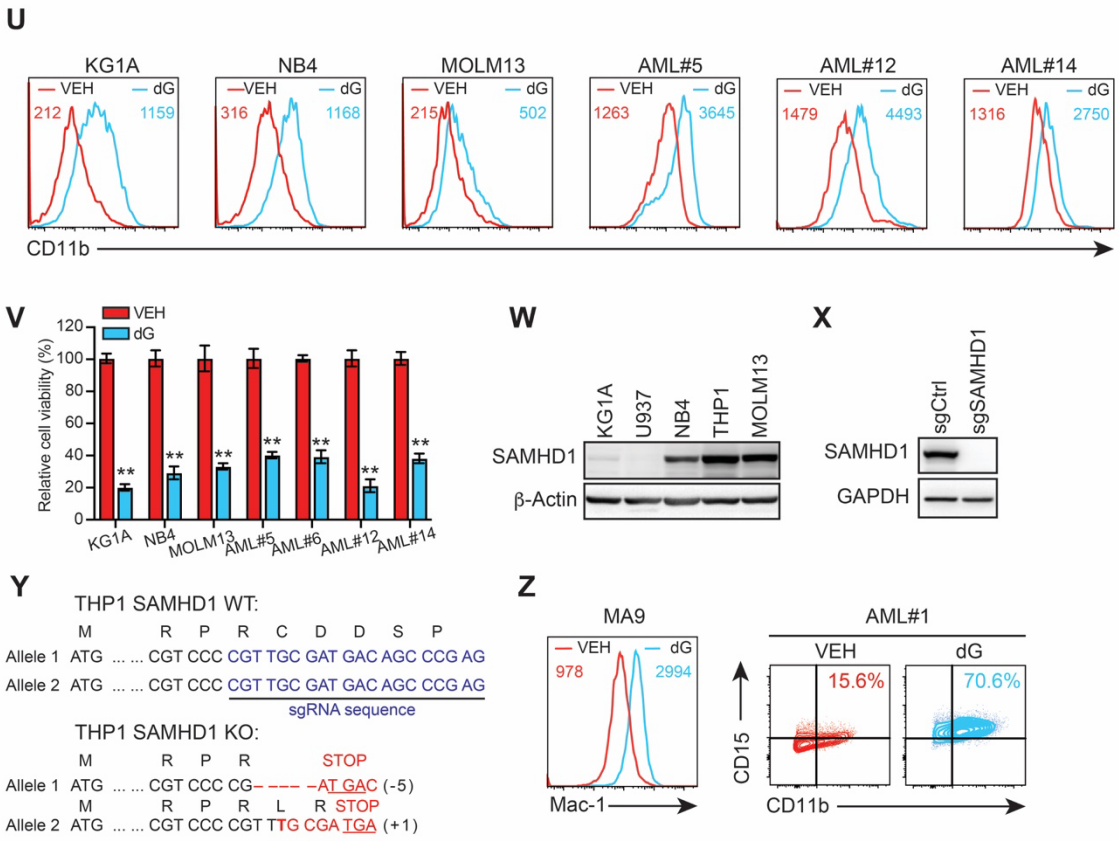
U
KG1A
NB4
MOLM13
AML#5
AML#12
AML#14
VEH
dG
212
1159
316
1168
215
502
1263
3645
1479
4493
1316
2750
CD11b
V
VEH
dG
Relative cell viability (%)
120
100
80
60
40
20
0
**
KG1A
NB4
MOLM13
AML#5
AML#6
AML#12
AML#14
W
KG1A
U937
NB4
THP1
MOLM13
SAMHD1
β-Actin
X
sgCtrl
sgSAMHD1
SAMHD1
GAPDH
Y
THP1 SAMHD1 WT:
M R P R C D D S P
Allele 1 ATG ... ... CGT CCC CGT TGC GAT GAC AGC CCG AG
Allele 2 ATG ... ... CGT CCC CGT TGC GAT GAC AGC CCG AG
sgRNA sequence
THP1 SAMHD1 KO:
M R P R STOP
Allele 1 ATG ... ... CGT CCC CG– ––– –AT GAC (-5)
M R P R L R STOP
Allele 2 ATG ... ... CGT CCC CGT TTG CGA TGA (+1)
Z
MA9
VEH
dG
978
2994
Mac-1
AML#1
VEH
dG
15.6%
70.6%
CD15
CD11b

Figure S2. NEL's differentiation-induction is caused by dNTPs imbalance (Related to Figure 2)

(A) The metabolic trajectory of NEL. NEL is first demethylated to Ara-G by adenosine deaminase (ADA), then phosphorylated into Ara-GMP by deoxycytidine kinase (DCK) or deoxyguanosine kinase (DGK), which is a rate-limiting step. Next, nucleoside monophosphate kinase (NMPK) and nucleoside diphosphate kinase (NDPK) convert Ara-GMP to Ara-GTP sequentially. SAMHD1 limits Ara-GTP cytotoxicity by hydrolyzing Ara-GTP, preventing its misincorporation into genomic DNA.

(B) Representative chromatograms of Ara-GTP and GTP in U937 (blue) or THP1 (red) cells following NEL treatment (10 μM, 12 hours).

(C) Intracellular dNTP or dNDP levels were quantified relative to their NTP or NDP counterparts in U937 (left) or KG1A cells (right) following NEL treatment (10 μM, 12 hours). Results represent the mean ± SEM. * P<0.05 and ** P<0.01.

(D) Fractional labeling of indicated deoxynucleotides in vehicle- or NEL-treated U937 cells cultured in media containing amide-^{15}N-labeled glutamine for 12 hours. The color indicates different isotopologues. Data from quadruplicates were normalized to total amounts of individual deoxynucleotides and represented as the mean ± SEM.

(E) Representative chromatograms of dGDP vs. ADP, Ara-CTP vs. CTP, dGTP vs. ATP, Ara-GTP vs. GTP in charcoal depleted cells.

(F) U937 cells were treated with vehicle, NEL (10 μM), COH29 (10 μM), or combination for 12 hours and intracellular dNTP levels were quantified by primer extension assay. Numbers denote the fold changes relative to vehicle-treated controls. Results represent the mean ± SEM, and ** P<0.01.

(G) Cell cycle analysis by Ki67/DAPI labeling in U937 cells at indicated time points post double aphidicolin (APD) block. Asynchronous cells (AS) were served as control.

(H) Intracellular dNTP levels of asynchronous (AS) U937 cells versus synchronous U937 cells enriched at S phase (S, 5 hours post double APD block) were quantified by primer extension assay. Numbers denote the fold changes relative to asynchronous cells. Results represent the mean ± SEM, and * P<0.05.

(I) Intracellular dNTP levels of U937 cells treated with COH29 (10 μM) for 48 hours were quantified by primer extension assay. Numbers denote the fold changes relative to vehicle-treated controls. Results represent the mean ± SEM, and ** P<0.01.

(J) CD11b expression levels in U937 cells treated with vehicle, COH29 (10 μM) for 48 hours and 96 hours.

(K) Relative cell viability of U937 cells treated with vehicle, NEL (10 μM), COH29 (10 μM) or combination for 96 hours. Results represent the mean ± SEM. ns, non-significant, and ** *P*<0.01.
(L) Relative cell viability of primary AML $CD34^+$ cells from patient specimens (AML#1, AML#7, AML#8), and normal $CD34^+$ cells from healthy donors (two PBSCs and one cord blood), treated with vehicle or COH29 as indicated for 96 hours. Results represent the mean ± SEM. ns, non-significant.
(M) Cell cycle analysis by Ki67/DAPI labeling in ishCtrl- and ishRRM2-U937 cells following doxycycline induction.
(N) Intracellular dNTP levels of ishCtrl- and ishRRM2-U937 cells treated with vehicle or NEL (10 μM, 12 hours), following doxycycline induction. Numbers denote the fold changes relative to vehicle-treated controls. Results represent the mean ± SEM, and ** *P*<0.01.
(O-P) CD38 expression levels (O) and relative cell viability (P) of ishCtrl- and ishRRM2-U937 cells with or without NEL treatment (10 μM, 96 hours), following doxycycline induction. Results represent the mean ± SEM, and ** *P*<0.01.
(Q) Apoptosis of U937 cells treated with vehicle or dG (10 μM, 48 hours). Results represent the mean ± SEM, and ** *P*<0.01.
(R) Intracellular dNTP levels of U937 cells treated with vehicle, dG (10 μM) or dG (10 μM) plus dC (10 μM) for 12 hours were quantified by primer extension assay. Numbers denote the fold changes relative to vehicle-treated controls. Results represent the mean ± SEM. * *P*<0.05, and ** *P*<0.01.
(S) Relative cell viability of U937 cells treated with vehicle, dG (10 μM), dG (10 μM) plus dA (10 μM), dG (10 μM) plus dC (10 μM) for 48 hours. Results represent the mean ± SEM, and ** *P*<0.01.
(T) Intracellular dGTP levels of U937 cells treated with vehicle, dG (10 μM), forodesine (1 μM) or combination for 12 hours were quantified by primer extension assay. Results represent the mean ± SEM, and ** *P*<0.01.
(U-V) CD11b expression levels (U) and relative cell viability (V) of indicated AML cells treated with vehicle or dG (KG1A, 10 μM; NB4, MOLM13, AML#5, AML#6, AML#12 and AML#14, 15 μM) for 48 hours. For (V), results represent the mean ± SEM, and ** *P*<0.01.
(W) Western blot of SAMHD1 levels in indicated AML cell lines.
(X) Western blot of SAMHD1 levels in Cas9-expressing THP1 cells transduced with lentiviral vectors expressing SAMHD1-directed sgRNA (sgSAMHD1) or non-targeting control (sgCtrl).
(Y) Genotyping of sgSAMHD1-THP1 cell clone demonstrates biallelic heterozygous truncations (-5bp/+1bp). sgRNA sequence is highlighted in blue.

(Z) Mac-1 expression levels in $MA9^+$ primary murine AML cells (left) and $CD11b^+/CD15^+$ subpopulation percentages in primary AML $CD34^+$ cells from specimen AML#1 (right) upon dG treatment (15 μM, 7 days).

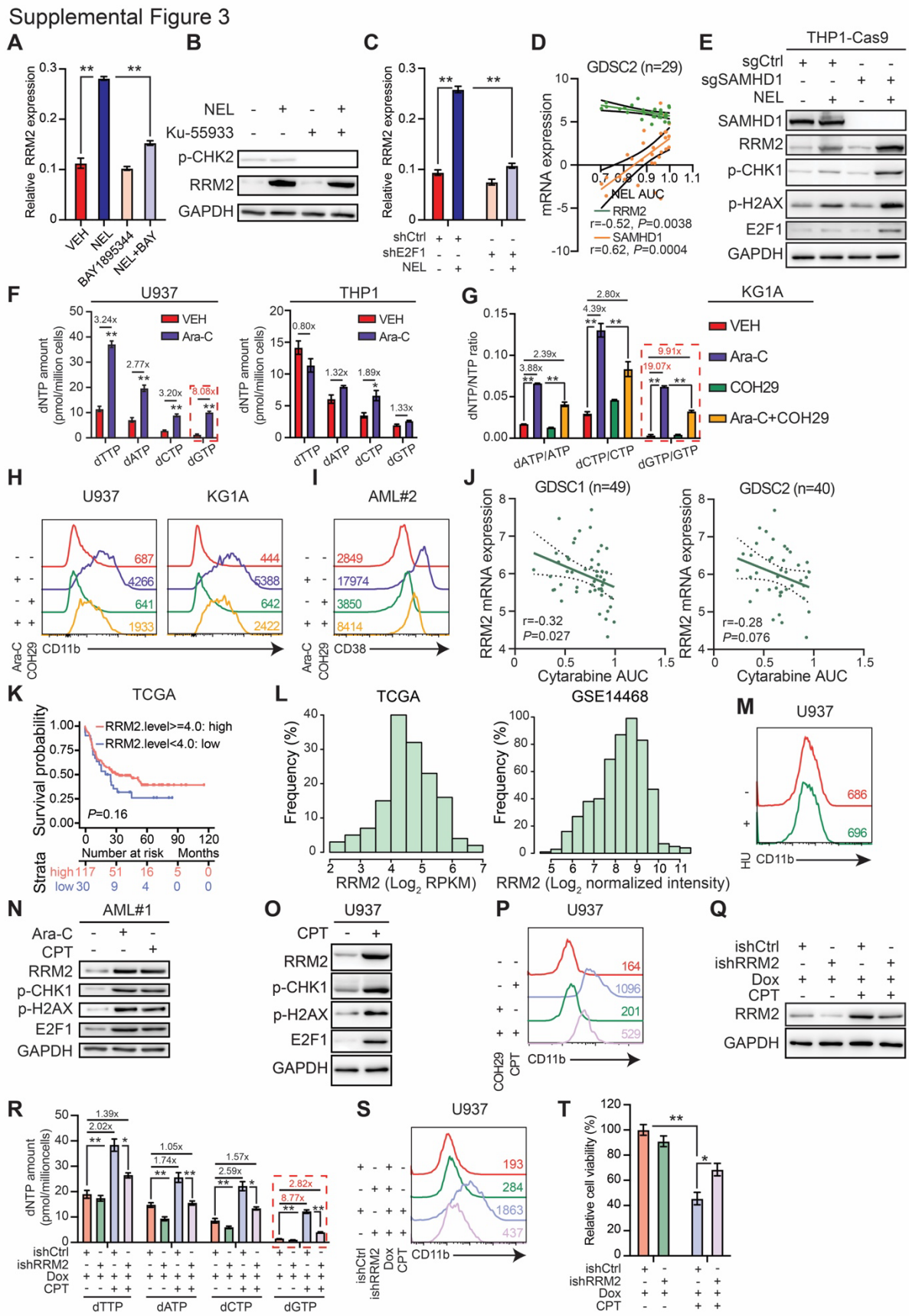
Supplemental Figure 3
A
Relative RRM2 expression
VEH
NEL
BAY1895344
NEL+BAY
B
NEL
Ku-55933
p-CHK2
RRM2
GAPDH
C
Relative RRM2 expression
shCtrl
shE2F1
NEL
D
GDSC2 (n=29)
mRNA expression
NEL AUC
RRM2
r=-0.52, P=0.0038
SAMHD1
r=0.62, P=0.0004
E
THP1-Cas9
sgCtrl
sgSAMHD1
NEL
SAMHD1
RRM2
p-CHK1
p-H2AX
E2F1
GAPDH
F
U937
THP1
dNTP amount (pmol/million cells)
VEH
Ara-C
dTTP
dATP
dCTP
dGTP
G
KG1A
dNTP/NTP ratio
VEH
Ara-C
COH29
Ara-C+COH29
dATP/ATP
dCTP/CTP
dGTP/GTP
H
U937
KG1A
Ara-C
COH29
CD11b
I
AML#2
CD38
J
GDSC1 (n=49)
GDSC2 (n=40)
RRM2 mRNA expression
r=-0.32
P=0.027
r=-0.28
P=0.076
Cytarabine AUC
K
TCGA
Survival probability
RRM2.level>=4.0: high
RRM2.level<4.0: low
P=0.16
Number at risk
Months
Strata
high
low
L
TCGA
GSE14468
Frequency (%)
RRM2 (Log2 RPKM)
RRM2 (Log2 normalized intensity)
M
U937
HL
CD11b
N
AML#1
Ara-C
CPT
RRM2
p-CHK1
p-H2AX
E2F1
GAPDH
O
U937
CPT
RRM2
p-CHK1
p-H2AX
E2F1
GAPDH
P
U937
COH29
CPT
CD11b
Q
ishCtrl
ishRRM2
Dox
CPT
RRM2
GAPDH
R
dNTP amount (pmol/millioncells)
ishCtrl
ishRRM2
Dox
CPT
dTTP
dATP
dCTP
dGTP
S
U937
ishCtrl
ishRRM2
Dox
CPT
CD11b
T
Relative cell viability (%)
ishCtrl
ishRRM2
Dox
CPT

Figure S3. Replication stress signaling mediated RRM2 upregulation is responsible for myeloid differentiation (Related to Figure 3)

(A) Relative RRM2 mRNA expression levels in U937 cells treated with vehicle, NEL (10 μM), BAY1895344 (50 nM) or combination for 12 hours. Results represent the mean ± SEM, and ** P<0.01.

(B) Western blot of the indicated proteins in U937 cells treated with vehicle, NEL (10 μM), Ku-55933 (2 μM) or combination for 12 hours.

(C) Relative RRM2 mRNA expression levels in U937 cells transduced with shRNA against E2F1 (shE2F1) or scramble control (shCtrl) after NEL treatment (10 μM) for 12 hours. Results represent the mean ± SEM, and ** P<0.01.

(D) Pearson correlation of RRM2 and SAMHD1 mRNA expression levels with NEL sensitivity in a panel of 29 hematopoietic cell lines. AUC, area under the curve. Data were sourced from GDSC2 portal.

(E) Western blot of the indicated proteins in sgCtrl- and sgSAMHD1-THP1 cells treated with NEL (20 μM) for 12 hours.

(F) Intracellular dNTP levels of U937 (left) and THP1 (right) cells treated with vehicle or Ara-C (0.5 μM) for 12 hours were quantified by primer extension assay. Numbers denote the fold changes relative to vehicle-treated controls. Results represent the mean ± SEM. * P<0.05 and ** P<0.01.

(G) KG1A cells were treated with vehicle, Ara-C (0.5 μM), COH29 (10 μM), or combination for 12 hours, and intracellular dNTP levels were quantified relative to their NTP counterparts by HPLC/MS. Numbers denote the fold changes of dNTP/NTP ratios relative to vehicle-treated controls. Results represent the mean ± SEM, and ** P<0.01.

(H-I) CD11b expression levels in U937 and KG1A cells (H) or CD38 expression levels in primary AML $CD34^+$ cells from specimen AML#2 (I) treated with vehicle, Ara-C (0.5 μM), COH29 (10 μM), or combination for 96 hours.

(J) Pearson correlation of RRM2 mRNA expression levels with Ara-C sensitivity in a panel of 49 hematopoietic cell lines from GDSC1 (left) and 40 hematopoietic cell lines from GDSC2 (right). AUC, area under the curve.

(K) Kaplan-Meier survival analysis of a cohort of patients with AML (TCGA) after dichotomization for RRM2 mRNA levels below (blue, n =30) and above (red, n = 117) 4.0 on a $\log_2$ (RPKM) scale (P=0.16).

(L) Histograms showing RRM2 mRNA expression levels in AML blasts at diagnosis from the patient cohorts of TCGA (left) and GSE14468 (right).

(M) CD11b expression levels in U937 cells treated with vehicle or HU (20 μM) for 96 hours.
(N) Western blot of the indicated proteins in primary AML $CD34^+$ cells from specimen AML#1 treated with vehicle, Ara-C (0.5 μM) or CPT (20 nM) for 12 hours.
(O) Western blot of the indicated proteins in U937 cells treated with vehicle or CPT (20 nM) for 12 hours.
(P) CD11b expression levels in U937 cells treated with vehicle, CPT (20nM), COH29 (10 μM), or combination for 96 hours.
(Q) Western blot of the indicated proteins in ishCtrl- and ishRRM2-U937 cells treated with vehicle or CPT (20 nM, 12 hours), following doxycycline induction.
(R) Intracellular dNTP levels of ishCtrl- and ishRRM2-U937 cells treated with vehicle or CPT (20 nM, 12 hours), following doxycycline induction. Numbers denote the fold changes relative to vehicle-treated controls. Results represent the mean ± SEM. * $P<0.05$ and ** $P<0.01$.
(S-T) CD11b expression levels (S) and relative cell viability (T) of ishCtrl- and ishRRM2-U937 cells with or without CPT treatment (20 nM, 96 hours), following doxycycline induction. Results represent the mean ± SEM. * $P<0.05$ and ** $P<0.01$.

Supplemental Figure 4

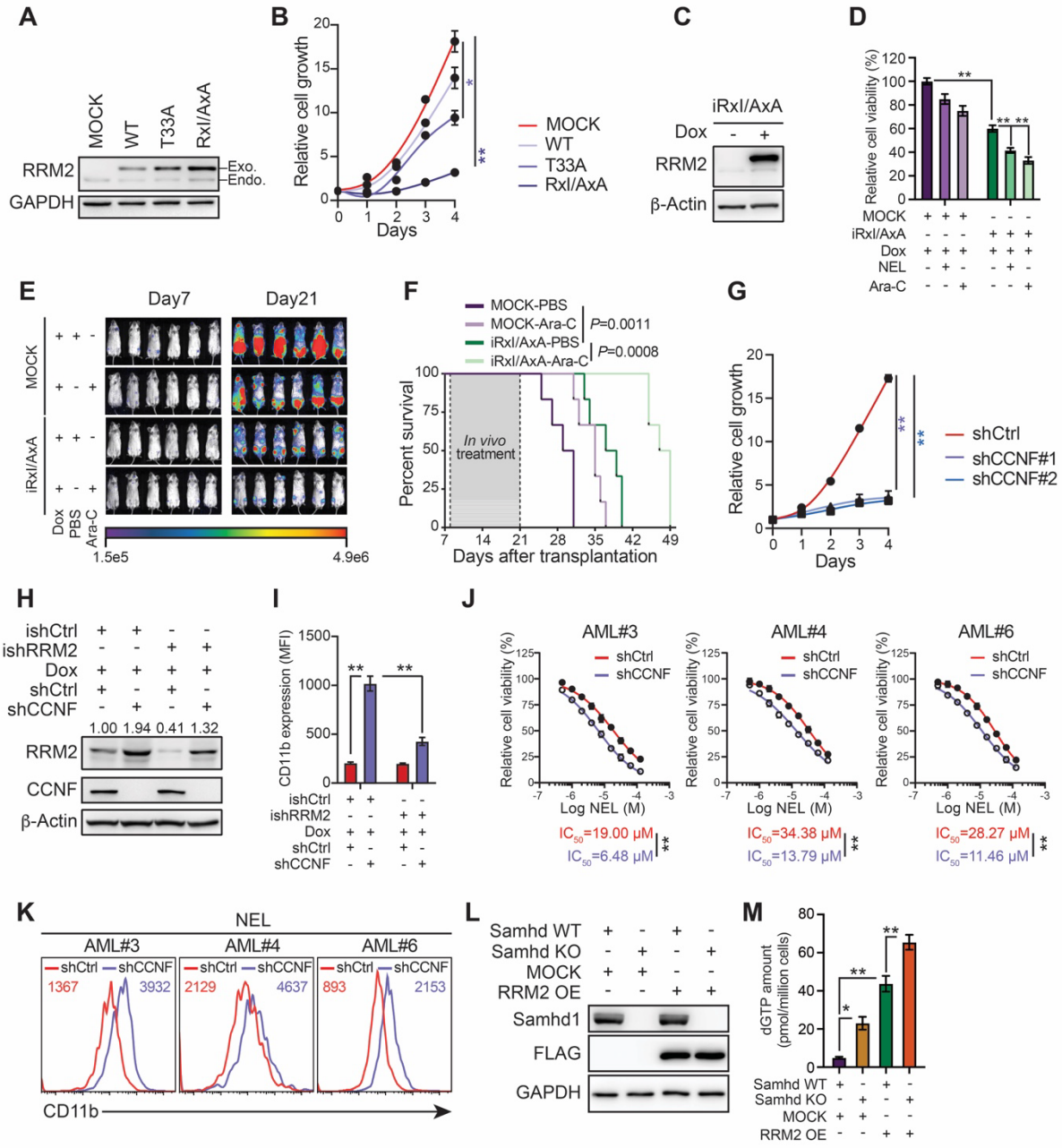

Figure S4. Genetically elevating RRM2 levels impairs AML maintenance (Related to Figure 4)

(A) Western blot of RRM2 protein levels in the selected THP1 cells ectopically expressing empty vector (MOCK) or indicated RRM2 variants. WT, RRM2 WT construct; T33A, RRM2 Thr33 to Ala point mutation, RRM2 phosphorylation-deficient construct; Rxl/AxA, RRM2 CCNF binding-deficient construct. Rxl motif, located at residues aa49-aa51, reportedly binding to cyclin F, was mutated to AxA.

(B) Relative cell growth of THP1 cells transduced with empty vector (MOCK) or indicated RRM2 variants. Results represent the mean ± SEM. * P<0.05 and ** P<0.01.

(C) Western blot of RRM2 protein levels in THP1 cells engineered with inducible RRM2-Rxl/AxA mutant construct (iRxl/AxA) with or without doxycycline induction (2 μg/mL).

(D) Relative cell viability of MOCK- or iRxl/AxA-THP1 cells treated with vehicle, NEL (20 μM) or Ara-C (0.5 μM) for 96 hours, following DOX induction. Results represent the mean ± SEM, and ** P<0.01.

(E-F) Engineered THP1 cells (1×10^6 cells per mouse) were injected into NSGS mice. Following engraftment, two groups of mice receiving either MOCK cells or iRxl/AxA cells were treated with DOX (i.g., 10 mg/kg, daily). In MOCK or iRxl/AxA transplants, mice were divided into two treatment groups injected with either vehicle (PBS) or Ara-C (i.p., 50 mg/kg, daily) (n=6 per group), and then assessed for engraftment by bioluminescence imaging (E) or monitored for survival (F).

(G) Relative cell growth of THP1 cells transduced with shCtrl, shCCNF#1 or shCCNF#2 lentivirus. Results represent the mean ± SEM, and ** P<0.01.

(H-I) Western blot of the indicated proteins (H) and CD11b expression levels (I) in ishCtrl- and ishRRM2-THP1 cells with or without CCNF knockdown after doxycycline induction. Lentivirus-mediated CCNF knockdown (shCCNF with RFP co-expression) was performed 2 days after doxycycline induction; additional 2 days later, RFP^+ cells were sorted for western blot analysis or CD11b assessment. For western blot, engineered cells were enriched for G_2/M populations by treatment with nocodazole (100 ng/mL, 16 hours). For (I), results represent the mean ± SEM, and ** P<0.01.

(J) Primary AML $CD34^+$ cells (n=3) were transduced with shCtrl or shCCNF lentivirus prior to viability inhibition assay for 96 hours in the presence of NEL at the indicated concentrations. The IC_{50} values between cells transduced with shCtrl lentivirus and their shCCNF counterparts were analyzed by means of Extra-sum-of-squares F test. Results represent the mean ± SEM, and ** P<0.01.

(K) CD11b expression levels in primary AML $CD34^+$ cells (n=3) transduced with shCtrl or shCCNF lentivirus and further treated with NEL (20 μM, 96 hours).

(L-M) Western blot of the indicated proteins (L) and primer extension assay of intracellular dGTP levels (M) in $CD45.2^+$ donor cells sorted from BM of $CD45.1^+$ congenic recipients transplanted with engineered $MA9^+$ murine AML cells as indicated. Results represent the mean ± SEM. * $P<0.05$, and ** $P<0.01$.

Supplemental Figure 5

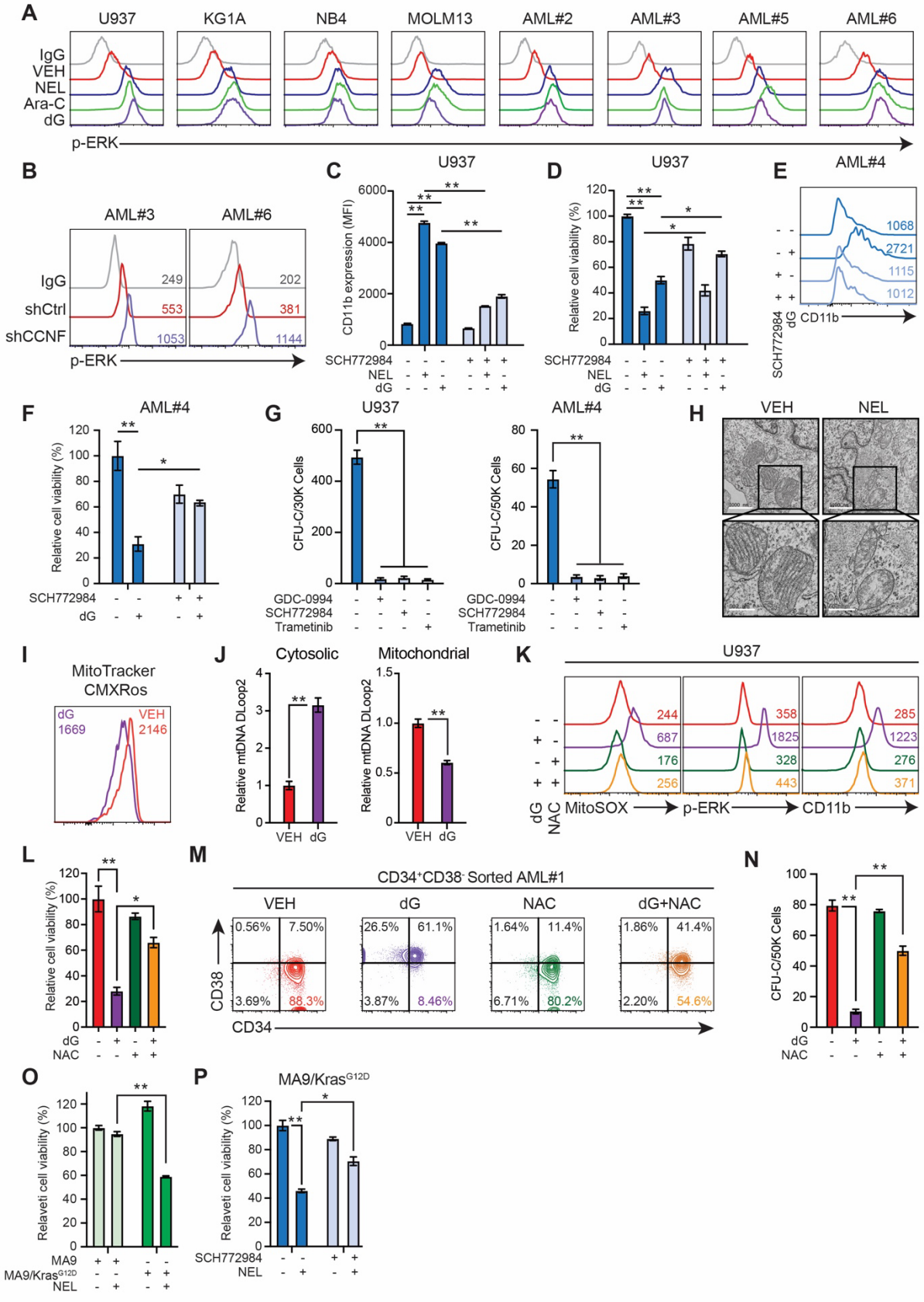

Figure S5. ERK activation contributes to myeloid differentiation (Related to Figure 5)

(A) Phospho-ERK levels in indicated AML cells treated with vehicle, NEL (10 μM for U937 and KG1A, 20 μM for NB4, MOLM13, AML#2, AML#3, AML#5 and AML#6), Ara-C (0.5 μM) or dG (10 μM for U937 and KG1A, 15 μM for NB4, MOLM13, AML#2, AML#3, AML#5 and AML#6) for 24 hours.

(B) Phospho-ERK levels in primary AML $CD34^+$ cells from specimen AML#3 or AML#6 transduced with shCtrl or shCCNF lentivirus.

(C-D) CD11b expression levels (C) and relative cell viability (D) of U937 cells pretreated with SCH772984 (2 μM) for 6 hours, followed by treatment with NEL (10 μM, 96 hours) or dG (10 μM, 48 hours). Results represent the mean ± SEM. * P<0.05, and ** P<0.01.

(E-F) CD11b expression levels (E) and relative cell viability (F) of primary AML $CD34^+$ cells from specimen AML#4 pretreated with SCH772984 (2 μM) for 6 hours, followed by treatment with dG (15 μM, 48 hours). Results represent the mean ± SEM. * P<0.05, and ** P<0.01.

(G) CFC assay of U937 cells (left) and primary AML $CD34^+$ cells from specimen AML#4 (right) treated with ERK inhibitor GDC-0994 (5 μM), ERK inhibitor SCH772984 (2 μM) or MEK inhibitor trametinib (30 nM) for 7 days. Results represent the mean ± SEM, and ** P<0.01.

(H) Transmission electron microscopy images of mitochondrial cristae in U937 cells treated with vehicle or NEL (10 μM) for 24 hours. Scale bar, 1 μm (upper panel) or 0.5 μm (lower panel).

(I) Flow cytometry analyses of mitochondrial membrane potential in U937 cells treated with vehicle or dG (10 μM) for 24 hours.

(J) Relative mtDNA DLoop2 abundance within cytoplasm (left) or mitochondria (right) of U937 cells treated with vehicle or dG (10 μM) for 24 hours. Results represent the mean ± SEM, and ** P<0.01.

(K-L) Mitochondrial superoxide levels, phospho-ERK levels, CD11b expression levels (K) and relative cell viability (L) of U937 cells treated with vehicle, dG (10 μM), NAC (2 mM) or combination. Mitochondrial superoxide and phospho-ERK analyses were performed after treatment for 24 hours. CD11b expression and cell viability analyses were performed after treatment for 96 hours. For (L), results represent the mean ± SEM. * P<0.05 and ** P<0.01.

(M) CD34 and CD38 level changes of $CD34^+CD38^-$ subset from primary AML cells (AML#1) treated with vehicle, dG (15 μM), NAC (2 mM) or combination for 48 hours.

(N) CFC assay of $CD34^+CD38^-$ AML cells (AML#1) treated as indicated in (M) for 7 days. Results represent the mean ± SEM, and ** P<0.01.

(O) Relative cell viability of murine $MA9^+$ and $MA9/Kras^{G12D}$ cells treated with vehicle or NEL (20 μM) for 96 hours. Results represent the mean ± SEM, and ** P<0.01.

(P) Relative cell viability of murine MA9/Kras^{G12D} cells pretreated with SCH772984 (2 μM) for 6 hours, followed by treatment with NEL (20 μM) for 96 hours. Results represent the mean ± SEM. * P<0.05 and ** P<0.01.

Supplemental Figure 6

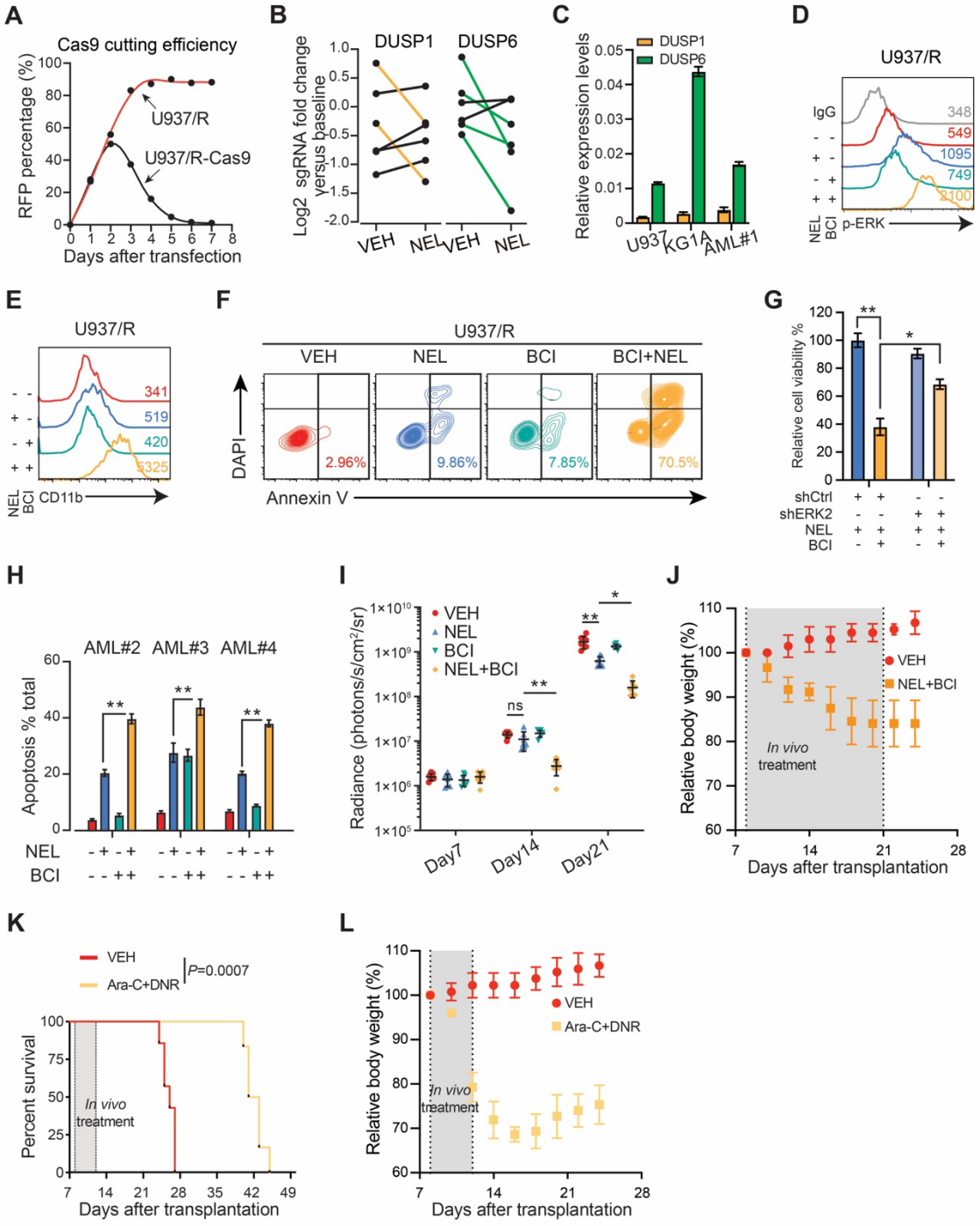

Figure S6. A loss-of-function screen identified synthetic lethal interaction between DUSP6-KO and nelarabine treatment (Related to Figure 6)

(A) Gene-editing efficiency of Cas9-expressing U937/R cells was validated by transduction with a lentiviral self-excising tag-RFP sgRNA construct. Lower percentage of RFP^+ cell population indicates higher Cas9 cleavage efficiency.

(B) Relative abundance of sgRNAs against either DUSP1 or DUSP6 in U937/R cells treated with vehicle or NEL, assessed by sequencing.

(C) Relative basal gene expression levels of DUSP1 and DUSP6 in indicated AML cells, assessed by RNA-seq.

(D) Phospho-ERK levels in U937/R cells treated with vehicle, NEL (20 μM), BCI (1 μM) or combination for 24 hours.

(E-F) CD11b expression levels (E) and apoptosis (F) of U937/R cells treated with vehicle, NEL (20 μM), BCI (1 μM) or combination for 96 hours.

(G) Relative cell viability of shCtrl- or shERK2-U937/R cells treated with NEL (20 μM) alone or NEL (20 μM) plus BCI (1 μM) for 96 hours. Results represent the mean ± SEM. * $P<0.05$ and ** $P<0.01$.

(H) Apoptosis of primary AML $CD34^+$ cells (n=3) treated with vehicle, NEL (20 μM), BCI (1 μM), or combination for 96 hours. Results represent the mean ± SEM, and ** $P<0.01$.

(I-J) MOLM13-luciferase cells (1×10^6 cells per mouse) were injected into sub-lethally irradiated NSGS mice. Following engraftment, mice were treated with vehicle (PBS), NEL (217 mg/kg, i.v., daily), BCI (10 mg/kg, i.p., daily), or combination for two weeks (n=7 per group). Quantitative bioimaging results on day 7, 14, 21 after transplantation (I), and relative mice body weight upon in-vivo combinatorial drug administration are shown (J). Results represent the mean ± SEM. ns, non-significant, * $P<0.05$ and ** $P<0.01$.

(K-L) MOLM13-luciferase cells (1×10^6 cells per mouse) were injected into sub-lethally irradiated NSGS mice. Following engraftment, mice were treated with vehicle (PBS), or the standard chemotherapy regimen consisting of a daily dose of 50 mg/kg Ara-C (i.p.) for five consecutive days along with a daily dose of 3 mg/kg DNR (i.v.) during the first three days of Ara-C treatment. Survival (K) and relative mice body weight upon in-vivo drug administration (L) are shown. For (L), results represent the mean ± SEM.